Electronic Supplementary Information for

Cobalt Nitrides as a class of Metallic Electrocatalysts for the Oxygen Evolution Reaction

Pengzuo Chen,[§a] Kun Xu,[§a] Yun Tong,[a] Xiuling Li,[a,c] Shi Tao,[b] Zhiwei Fang,[a] Wangsheng Chu,[b] Xiaojun Wu[a,c] and Changzheng Wu*[a]

[a] Hefei National Laboratory for Physical Sciences at Microscale, iChEM (Collaborative Innovation Center of Chemistry for Energy Materials), Hefei Science Center (CAS) and CAS Key Laboratory of Mechanical Behavior and Design of Materials, University of Science and Technology of China, Hefei, 230026, P. R. China.

[c] National Synchrotron Radiation Laboratory, University of Science and Technology of China, Hefei, Anhui 230029, PR China

[c] CAS Key Laboratory of Materials for Energy Conversion and Department of Material Science and Engineering, University of Science and Technology of China, Hefei, 230026, P. R. China

To whom correspondence should be addressed. E-mail: czwu@ustc.edu.cn

Table of contents

Table S1 Information of crystal structures for the serial cobalt nitrides

Phase	Crystal system	Space group	Unit cell
Co_2N	Orthorhombic	Pnnm (58)	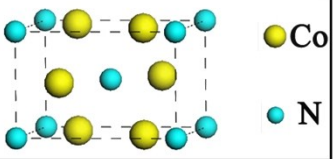
Co_3N	Hexagonal	P63/mmm (182)	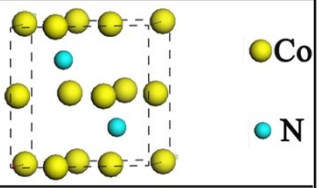
Co_4N	Cubic	Pm−3m (221)	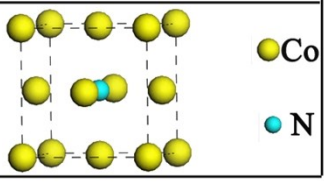

S2. The calculated density of states (DOS) of serial cobalt nitrides

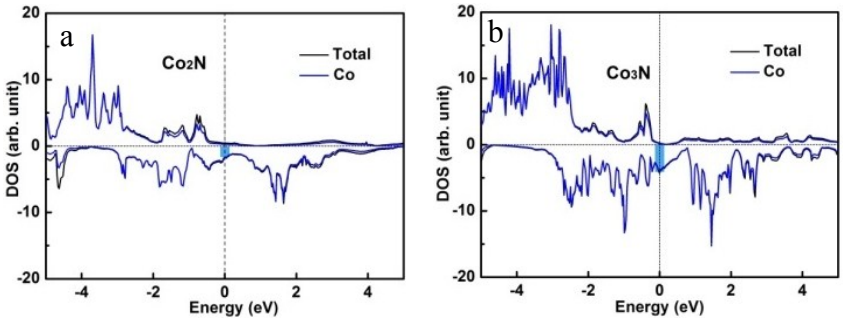

Figure S2 DOS diagrams of a) Co_2N and b) Co_3N catalysts.

S3. XRD patterns and SEM images of the α-$Co(OH)_2$ and β-$Co(OH)_2$ precursors

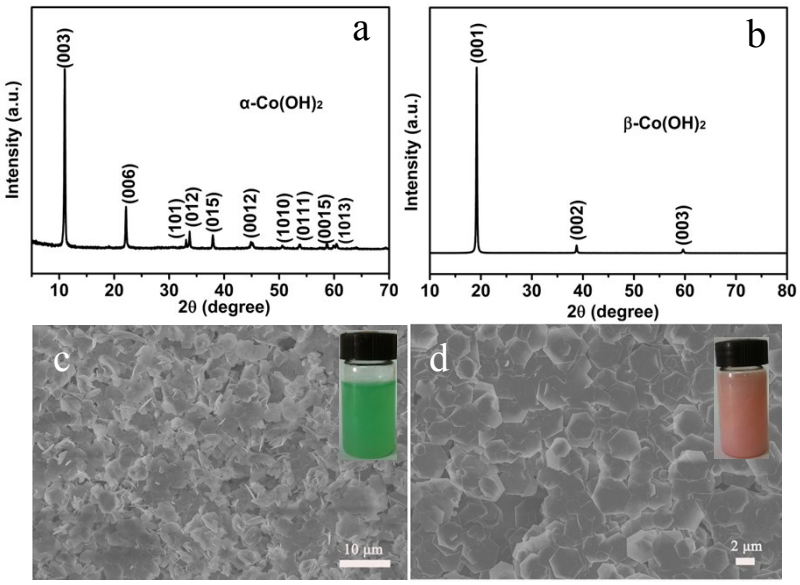

Figure S3 Characterizations of the α-$Co(OH)_2$ and β-$Co(OH)_2$ precursors. a, b) XRD patterns and c, d) SEM images. Inset: photographs of α-$Co(OH)_2$ (green) and β-$Co(OH)_2$ (pink).

As shown by XRD patterns in Figure S3a, b, the obtained intermediate precursors (α-$Co(OH)_2$ and β-$Co(OH)_2$) were all pure phases, exhibiting highly c-axis orientation. TEM images of the α-$Co(OH)_2$ and β-$Co(OH)_2$ in Figure S3c, d shows hexagonal nanosheets morphology with several micrometers. The inset photographs of α-$Co(OH)_2$ and β-$Co(OH)_2$ precursors display the obvious different colour. (α-$Co(OH)_2$ was green and β-$Co(OH)_2$ was pink).

S4. EELS spectrum and element mapping images of obtained Co_2N product

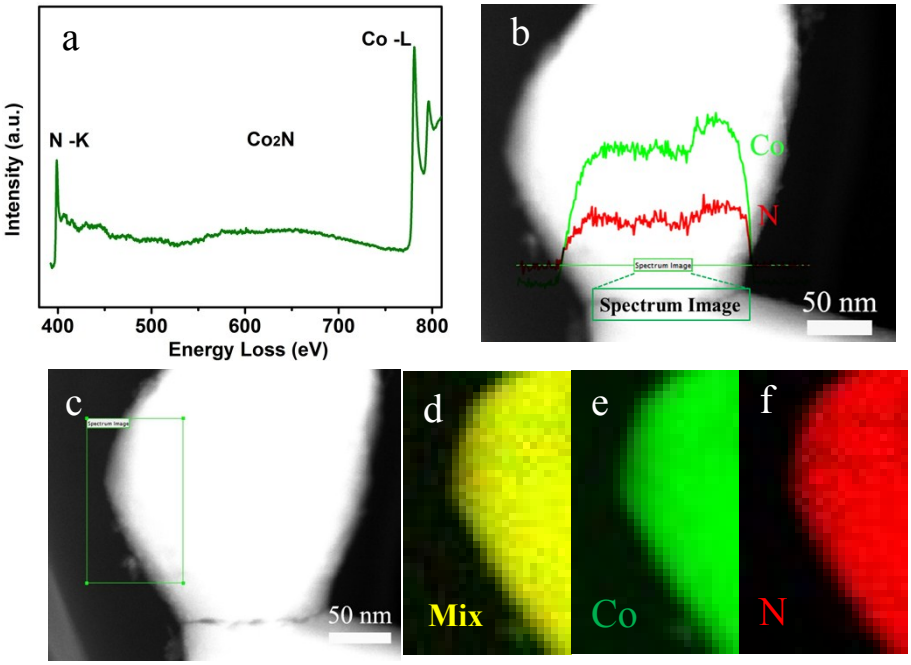

Figure S4 a) Electron energy loss spectroscopy (EELS) of obtained Co_2N product, b) EELS line scanning profiles of Co_2N, c) The typical HAADF-STEM and d-f) EELS element mapping images of Co_2N, where the elements of Co (indicated by green color) and N (indicated by red color) were homogenously spatial distributions, illustrated the successful synthesis of Co_2N.

S5. EELS spectrum and element mapping images of obtained Co_3N product

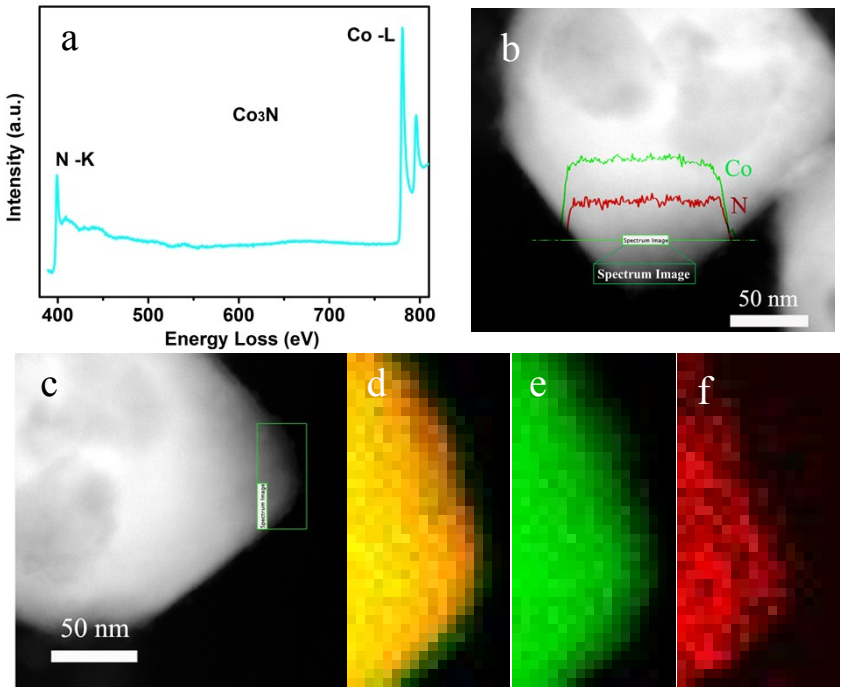

Figure S5 a) Electron energy loss spectroscopy (EELS) of obtained Co_3N product, b) EELS line scanning profiles of Co_3N, c) The typical HAADF-STEM and d-f) EELS element mapping images of Co_3N, where the elements of Co (indicated by green color) and N (indicated by red color) were homogenously spatial distributions, illustrated the successful synthesis of Co_3N.

S6. N_2 adsorption/desorption isotherms of serial cobalt nitrides

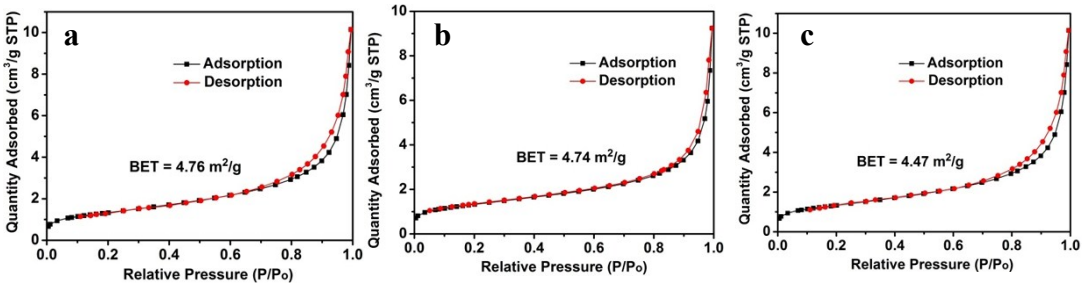

Figure S6 N_2 adsorption/desorption isotherms of (a) Co_2N, (b) Co_3N and (c) Co_4N samples.

S7. Polarization curves of metallic Co_4N catalyst with different loading weight

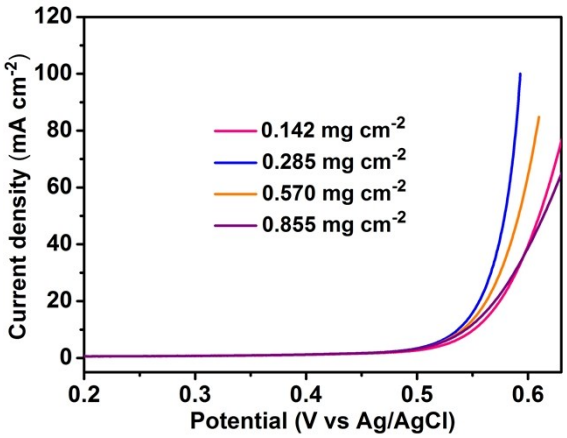

Figure S7 Polarization curves of metallic Co_4N catalyst with different loading weight in 1 M KOH solution.

S8. IR-corrected polarization curves for all of the catalysts after the BET surface area normalization

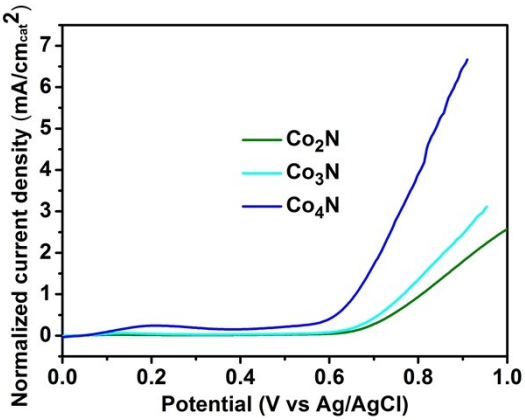

Figure S8 (a) IR-corrected polarization curves for Co_2N, Co_3N and Co_4N in a 0.1 M KOH medium. The current densities of all catalysts have been normalized by BET surface area.

S9. XPS spectrum of all catalysts after the prolonged electrocatalysis

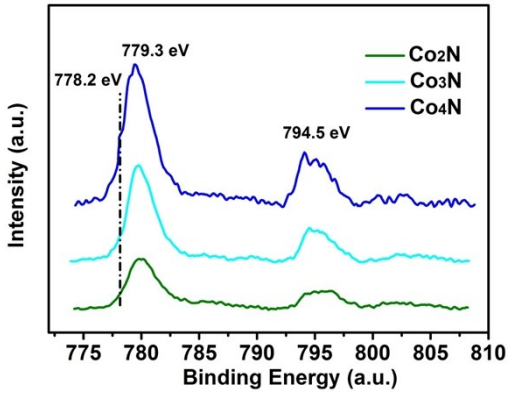

Figure S9 XPS spectrum of Co_2N, Co_3N and Co_4N catalysts after the prolonged electrocatalysis.

As well known, X-ray photoelectron spectroscopy (XPS) is very powerful for surface characterization. First of all, "post-mortem" XPS analysis has been performed to comprehend the surface change after prolonged CV tests. Figure S9 shows almost unanimous Co 2p spectrum of Co_2N, Co_3N and Co_4N catalysts after the prolonged electrocatalysis. The peaks located at 778.2 eV can be assigned to Co $2p_{3/2}$ of Co^0 in cobalt nitrides, which is identical with previous reports. Meanwhile, the peaks located at binding energy of 779.3 eV and 794.5 eV are consistent with Co^{2+} and Co^{3+}, demonstrating the existence of surface oxidation in cobalt nitrides catalysts after a long period of OER tests.

S10. XRD patterns of all catalysts after prolonged electrocatalysis

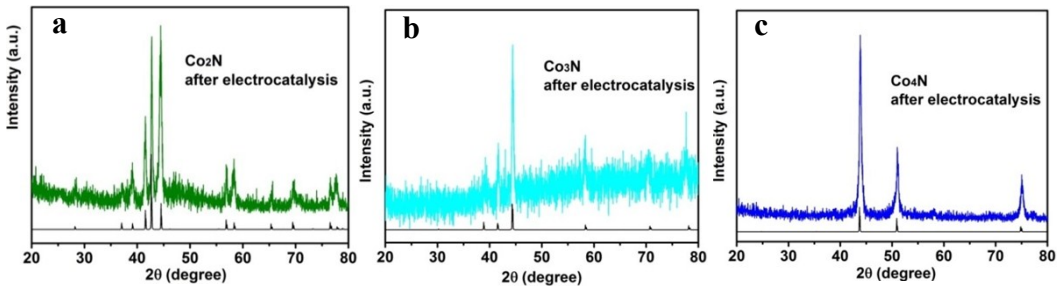

Figure S10 X-ray diffraction (XRD) patterns of a) Co_2N, b) Co_3N and c) Co_4N catalysts after the electrocatalysis

The XRD patterns in Figure S10 confirm all XRD curves of each compound after prolonged electrocatalytical measurement can be well indexed to the standard XRD profiles, indicating their excellent stability and phase stability after prolonged electrocatalysis process. Therefore, after prolonged OER tests, there is only a part of surface oxidation occurred in as-obtained cobalt nitrides as active phases, but it's still cobalt nitrides in bulk state, giving solid evidence that the major phase was always cobalt nitrides.

Table S2. Comparison of OER catalytic performance of bulk Co_4N to recently reported state of the art Co-based OER catalysts

Catalysts	*Overpotential @ 10 mA cm^{-2} (mV)*	*Tafel slope (mV dec^{-1})*	*Electrolyte*	*Substrate*	*Reference*
Bulk Co_4N	330	58	1 M KOH	Glassy carbon	This work
Ni-Co oxides amorphous layers	325	39	1 M NaOH	Glassy carbon	[1]
$NiCo_2(OH)_6$ nanotubes	460	65	0.1 M KOH	Self-support	[2]
Fe-Co_3O_4	486	/	0.1 M KOH	Glassy carbon	[3]
NG-$CoSe_2$ belt	366	40	0.1 M KOH	Glassy carbon	[4]
NiCo-LDH nanosheets	334	41	1 M KOH	Glassy carbon	[5]
$CoSe_2$ ultrathin nanosheets	320	44	0.1 M KOH	Glassy carbon	[6]
CoMn-LDH nanosheets	324	43	1 M KOH	Glassy carbon	[7]
N-graphene-CoO	340	71	1 M KOH	Glassy carbon	[8]
Co_3O_4/N-rmGO	310	67	1 M KOH	Glassy carbon	[9]
RuO_2	366	69	0.1 M KOH	Glassy carbon	[10]
IrO_2/C	310	/	0.1 M KOH	Glassy carbon	[11]

Reference

[1] Y. Yang, H. Fei, G. Ruan, C. Xiang and J. M. Tour, *ACS Nano* 2014, **8**, 9518.

[2] Z. Zhao, H. Wu, H. He, X. Xu and Y. Jin, *Adv. Funct. Mater.* 2014, **24**, 4698.

[3] T. Grewe, X. Deng and H. Tüysüz, *Chem. Mater.* 2014, **26**, 3162.

[4] M.-R. Gao, X. Cao, Q. Gao, Y.-F. Xu, Y.-R. Zheng, J. Jiang and S.-H. Yu, *ACS Nano* 2014, **8**, 3970.

[5] F. Song and X. Hu, *Nat Commun* 2014, **5**.

[6] Y. Liu, H. Cheng, M. Lyu, S. Fan, Q. Liu, W. Zhang, Y. Zhi, C. Wang, C. Xiao, S. Wei, B. Ye and Y. Xie, *J. Am. Chem. Soc*. 2014, **136**, 15670.

[7] F. Song and X. Hu, *J. Am. Chem. Soc.* 2014. **136**, 16481.

[8] S. Mao, Z. Wen, T. Huang, Y. Hou and J. Chen, *Energy Environ. Sci.* 2014, **7**, 609.

[9] Y. Liang, Y. Li, H. Wang, J. Zhou, J. Wang, T. Regier and H. Dai, *Nat Mater* 2011, **10**, 780.

[10] M.-R. Gao, X. Cao, Q. Gao, Y.-F. Xu, Y.-R. Zheng, J. Jiang and S.-H. Yu, *ACS Nano*, 2014, **8**, 3970.

[11] T. Y. Ma, S. Dai, M. Jaroniec and S. Z. Qiao, *J. Am. Chem. Soc*., 2014, **136**, 13925.